Temporal and spatial evolution of a waxing then waning catastrophic density current revealed by chemical mapping

Rebecca Williams*, Michael J. Branney, and Tiffany L. Barry
Department of Geology, University of Leicester, University Road, Leicester LE1 7RH, UK

ABSTRACT

We reconstruct the behavior of a catastrophic sustained radial pyroclastic density current as it waxed then waned during its brief lifespan. By subdividing the deposit into 8 time slices using a chemical tracer, we show that the sustained current initially was topographically restricted, but that its leading edge advanced in all directions, encroaching upon and gradually ascending hills. During peak flow the current reached its maximum extent and overtopped all topographic highs. After this, and while the current direction from source was maintained, the leading edge gradually retreated sourceward. High-resolution analysis of the depositional architecture reveals how the flow dynamics evolved and runout distance of the sustained density current rapidly increased then decreased, reflecting the dominant influence of changing mass flux, as demonstrated in numerical models but not previously distinguished in a natural deposit.

INTRODUCTION

Large particulate density currents are generally catastrophic and mostly not observed, so understanding of their flow dynamics derives from models and interpretations of deposits (Kneller and McCaffrey, 2003; Baas et al., 2004; Roche, 2012). They are the principal mode of sediment transport over ocean floors, they emplace ejecta blankets around bolide impact craters (Meyer et al., 2011; Branney and Brown, 2011), and they transport up to thousands of cubic kilometers of debris from explosive volcanoes (Self, 2006). They account for half of all deaths due to historic volcanic eruptions (Witham, 2005). Knowledge of how such currents respond to topography and changes in source flux is critical for the reconstruction of turbidite basin fills in hydrocarbon exploration (Plink-Björklund et al., 2001; Pirmez and Imran, 2003) and for anticipating hazards at volcanoes (Murcia et al., 2010). Simple models that involve instantaneous release of a prescribed volume as a single-surge flow (Dade and Huppert, 1996; Kelfoun, 2011) are not suitable for larger density currents that have sustained supply because in more sustained currents, flow velocity, thickness, concentration, mass flux, and direction may vary significantly with time; substrate topography changes during deposition (Brown and Branney, 2013); and only a small fraction of the ultimate deposit is being transported during any one snapshot in time (Bursik and Woods, 1996; Branney and Kokelaar, 1997). Meaningful inference of the dynamics of large natural currents, therefore, requires more sophisticated methods of interrogating the deposits than simply using the overall dimensions of the entire deposit sheet.

To reconstruct the history of a sustained current, its deposit must be divided into successive time slices. This is generally impossible in turbidites, because time slices are cryptic; bedding, lithofacies, or divisions tend to be diachronous (Kneller and McCaffrey, 2003). Distinctive tracers fed into a sustained current at certain times and then preserved at different levels within the resultant deposit are needed to delineate successive time surfaces, or "entrachrons" (Branney and Kokelaar, 2002). Some volcanoes satisfy this requirement, as the ejecta composition changes during sustained pyroclastic fountaining, which can persist for several hours (e.g., Carrasco-Núñez and Branney, 2005; Bachmann and Bergantz, 2008).

Compositional zoning has been used to reconstruct the successive stages of a protracted eruption that generated several ignimbrite and fallout layers (e.g., Fierstein and Wilson, 2005). In this paper we use compositional zoning to reconstruct at high resolution the history of a single, sustained density current that flowed radially from source. We use an exceptionally well exposed, topography-draping ignimbrite to reconstruct how the current behaved in all directions from source and as it surmounted topographic barriers. Cryptic (compositionally defined) entrachrons were carefully mapped in relation to geographic and topographic distribution in the landscape.

The Green Tuff Ignimbrite, Pantelleria

The ca. 45 ka Green Tuff ignimbrite on the island of Pantelleria (Italy) is a rare example of a near-circular ignimbrite that shows both gradational compositional zoning with height and superb exposure, allowing exceptional access to both longitudinal and lateral variations from source (Mahood and Hildreth, 1986). It forms a thin veneer (minimum volume estimate of 0.49 km^3) that covers the 83 km^2 island and drapes all topography, including both stoss and lee slopes, thickening from 30 cm to >10 m in paleovalleys (Orsi and Sheridan, 1984). Clast imbrication and flow lineations (Branney et al., 2004) show that the density current flowed radially outward from a central vent near the present caldera lake, where a precursory proximal pumice fall deposit is locally preserved (Fig. 1). The ignimbrite is a massive, very poorly sorted lapilli tuff with local gradations into diffuse-bedded and block-bearing facies (Fig. 1). Ubiquitous deposition rather than current bypassing (cf. Brown and Branney, 2004) was favored by the hot, sticky nature of the viscous particles that rapidly agglutinated to the substrate surface as the current passed (Branney et al., 2004), adhering to all slopes. Welding, the result of this hot emplacement, has preserved the clastic textures intact and prevented erosional stripping, even on steep (up to 85°) slopes, hence its remarkably complete preservation. Post-depositional rheomorphic modification is not extensive and has not obscured original sedimentary features.

Rapid emplacement of the zoned ignimbrite without significant pauses is inferred from the combination of evidence (Williams, 2010) including an absence of any remnant intercalated ashfall horizons; the gradational nature of the vertical compositional variations; analysis of the depositional lithofacies and grain fabrics; and the very simple vertical welding profile in which glassy upper and lower chilled zones enclose a welded interior that lacks internal chilled zones.

The topography at the time of the eruption was as it is today, except for a younger small volcano (V in Fig. 2); there were elevated inner and outer caldera rims (C1, C2), a shield-like hill in the south (H), and a gently sloping lava field in the northwest (Fig. 2).

METHOD

Close-spaced samples (≤20 cm) of more than 80 vertical sections were analyzed using X-ray fluorescence (XRF). A range of major and trace elements, such as Y and Nd, show systematic linear variation with height (Table DR1 in the GSA Data Repository[1]). The greatest degree of variation occurs in the immobile element Zr, which ranges from >2000 ppm near the base to <800 ppm near the top (Fig. 1). Detailed spot

*Current address: Department of Geography, Environment and Earth Sciences, University of Hull, Hull HU6 7RX, UK.

[1]GSA Data Repository item 2014030, Table DR1 (XRF analyses for the type section of the Green Tuff Formation), Table DR2 (LA-ICP-MS spot analyses of samples from the Green Tuff Formation type section), and Table DR3 (parameters selected for runout and duration calculations), is available online at www.geosociety.org/pubs/ft2014.htm, or on request from editing@geosociety.org or Documents Secretary, GSA, P.O. Box 9140, Boulder, CO 80301, USA.

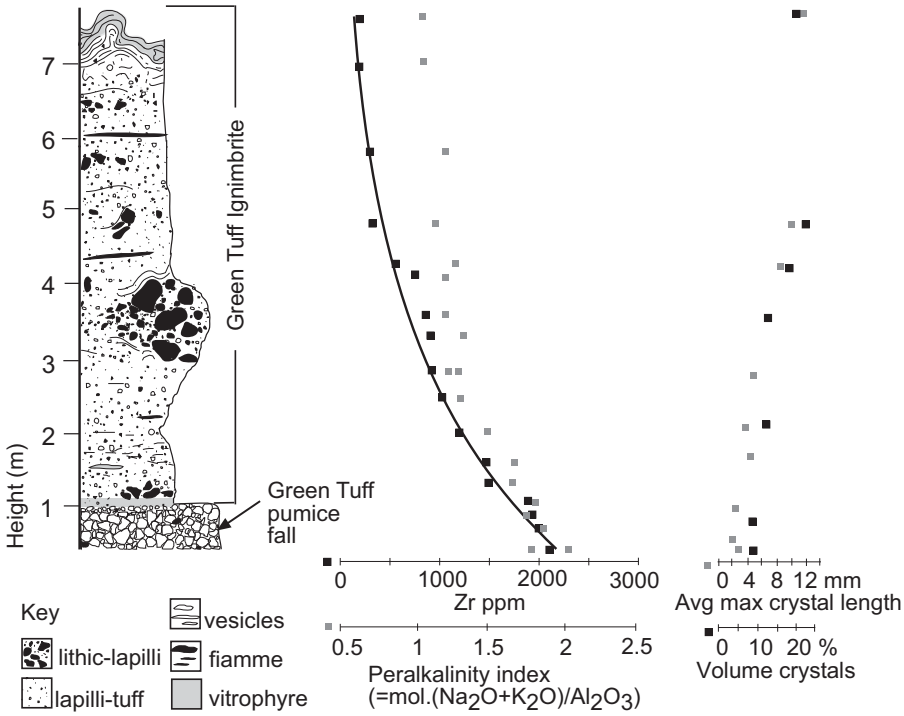

Figure 1. Vertical section of Green Tuff ignimbrite (Pantelleria, Italy), showing gradational compositional and mineralogical variations, with gradational variations in Zr values with height; 80 vertical sections logged for the study show similar variations. Deposit is mostly massive with well-preserved clastic textures. Upper parts typically show rheomorphic deformation.

analyses by electron microprobe (EMP) and laser ablation–inductively coupled plasma–mass spectrometry (LA-ICP-MS) show that this compositional trend occurs in both the glassy matrix and juvenile clasts (Table DR2). To facilitate the processing of a large sample set (n = 405) we used XRF analysis of whole rock samples after manual removal of lithic fragments.

Chemical Stratigraphy

The deposit shows a gradational compositional variation with height from pantellerite at the base to less-evolved trachyte at the top, matched by a gradual upward increase in the size and concentration of crystals (Fig. 1). This represents progressive tapping of a heterogeneous magma reservoir during the eruption (Mahood and Hildreth, 1986) that initially ejected crystal-poor magma enriched in incompatible elements whereas the later ejecta was less evolved, crystal rich, and poor in incompatible elements (Williams, 2010). Using Zr as a proxy, we subdivided the vertical variations into 200 ppm Zr zones at >80 sites (Fig. 3) and, using ArcGIS (www.esri.com/software/arcgis), mapped each zone in detail. This revealed a systematic change in geographic coverage by zones of the deposit (Fig. 2); the deposit distributions represent the changing footprint of the current during successive time intervals t_1 to t_8 (Fig. 2) as it gradually enveloped the island.

The Zr variation with height nowhere exhibits a reversal or departure from the overall linear compositional trend (Fig. 1), which confirms the steadily progressive nature of the current deposition. The boundaries of time slices (t_1–t_8) are gradational and cryptic (invisible at outcrop), and do not correspond with discernible compositional steps or marked grain-size or textural changes within what is predominantly a massive deposit layer (Williams, 2010). Thin, possible flow units occur locally just above the basal pumice fall layer (e.g., on the northern part of C1; Fig. 3), but they do not account for the zonation as all lie within the t_1 zone. They are interpreted to record small, local, precursory ephemeral currents prior to establishment of the main protracted density current.

RECONSTRUCTION OF THE CURRENT'S FLOW BEHAVIOR

The eruption began with localized pumice fallout from a low convective column (Fig. 1), followed by pyroclastic fountaining that generated an initially pulsing and then a sustained pyroclastic density current. This advanced radially across proximal areas of the inner caldera basin (t_1) and rapidly breached the northwest rim at one point, allowing a narrow tongue of the current to flow unrestricted to the sea. At this time, the current covered 47.3 km^2 and overtopped the inner caldera wall in the southeast, but not beyond the outer caldera wall, except at a narrow breach west of the shield volcano (H, Fig. 2). The current then gradually advanced to cover 61.1 km^2 (t_2), spreading further NNW, overtopping a steep, 221-m-high (differential height) scarp (Z) and inundating the low-lying northern part of the island. It also advanced farther east across parts of the caldera wall that had not previously been inundated and began to advance through a low, narrow breach in the outer caldera wall in the southeast. During t_3, the current continued to advance up the southern shield (H), but did not attain the summit. A small tongue

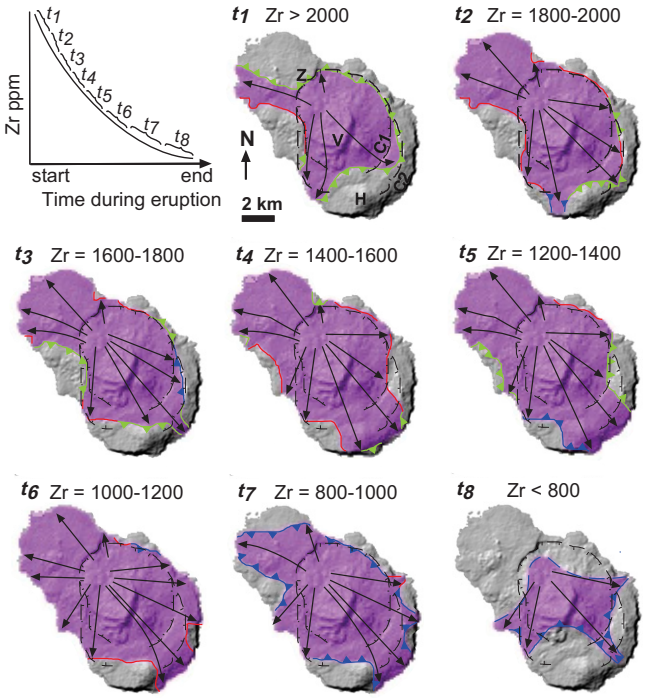

Figure 2. Changing distribution of sustained radial Green Tuff (Pantelleria, Italy) density current during eight time slices, t_1–t_8, as determined by detailed mapping of successive 200 ppm intervals of Zr in Green Tuff ignimbrite. Geographic footprint of protracted density current gradually increased and then gradually decreased as current waxed then waned. Arrows show inferred current directions. Current's distal limit variously advanced (green), remained stationary (red), and retreated sourceward (blue). Preexisting topographic barriers: H—shield-shaped hill (Cuddia Attalora); Z—Zinedi scarp; C1—an inner caldera rim (Monastero); C2—an outer caldera rim (La Vecchia). V—Montagna Grande, which post-dates density current. Location, data points, and spot heights are shown in Figure 3.

reached the sea east of the shield, while there was farther advance over the inner caldera wall in the east, but not yet the outer wall (at C2). By t_4, the current had extended widely (68.9 km^2); it passed over topographic barriers including wide sections of the main caldera scarps in the northeast and WSW and, finally, the summit region of the southern hill (H; 135 m differential height), while the inundation of the north of the island continued. During t_5 (70 km^2), the current crossed the southern coast and swept over the entire caldera scarp in the north, although flow to the east, WNW, and WSW remained restricted locally. By t_6, the current had inundated the entire island, with a few minor exceptions, and had flowed over and past the caldera scarps in both the east and west. Maximum coverage, 73.1 km^2, was during this time interval, but there are signs that the current had already started to wane; it had retreated from the summit of the shield (H), with flow being deflected around its eastern flank. By t_7, the area covered by the current was gradually decreasing (to 64.3 km^2) and the runout distance in several sectors was decreasing, particularly in the north. During t_8, the area covered by the current continued to decrease to 42.1 km^2, no longer reaching the north of the island and, once again, becoming restricted to proximal areas, with flow persisting longest toward the west and east.

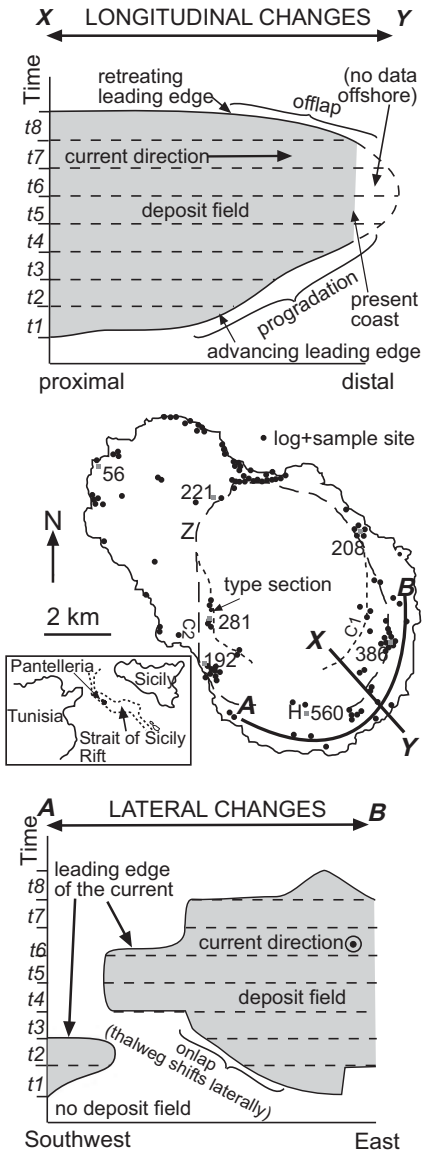

Figure 3. Time (t_1–t_8) versus distance plots for Green Tuff (Pantelleria, Italy) in longitudinal (X-Y) and circumferential (A-B; current coming out of page) sections, showing that base and top of deposit are diachronous, with onlap and offlap recording how current waxed (t_1–t_4) and then waned (t_6–t_8). Location map (center) shows distribution of data points and sections, and spot heights of topographic highs (in meters). In the south, current flow path shifted laterally as current waxed, recorded as lateral overlap from east to west (t_2–t_4). As current waned, it shifted eastward again (t_5–t_7) until only narrow finger of current persisted (t_8). Widespread preservation of original top surface of ignimbrite means that offlap relations are not just an artifact of subsequent erosion.

DISCUSSION: INTERPRETATION OF FLOW BEHAVIOR

We have shown that the leading edge of a radial density current progressively extended across a landscape and then gradually retreated from distal and then medial areas. The deposit architecture developed to have diachronous lower and upper surfaces (Fig. 3), which indicates that the geographic area covered by the current first increased, and then decreased with time. In addition, deposition locally progressed by lateral accretion, indicating that thalwegs within the current migrated laterally with time (Fig. 3). Rapidly shifting patterns of deposition during sustained radial pyroclastic density current activity have been inferred from deposits elsewhere (Brown and Branney, 2013), but the results of the present study reveal previously unknown emplacement dynamics and on a current-wide scale.

Sustained radial density currents are inherently depletive (Kneller and Branney, 1995) as the result of flow divergence, deposition during transport, and dilution by mixing with ambient fluid (Bursik and Woods, 1996). At a certain distance from source these combined effects cause the current to lift off from the ground and rise as a buoyant phoenix plume (Woods et al., 1998; Branney and Kokelaar, 2002), and this lift-off point represents the current's distal limit (Fig. 4). Experimental and numerical models show that this distance is largely controlled by the mass flux of the eruptive supply (Bursik and Woods, 1996), although it is also influenced by topography (Woods et al., 1998). During steady conditions, a constant runout distance is maintained. However, the runout distance of the Green Tuff density current varied with time (Fig. 3) and for much of its duration it did not reach its maximum runout distance. Therefore, it is useful to consider the runout distances reached by the current during the successive time intervals (t_1–t_8; Figs. 2 and 3).

We can assume that the eruption was waxing at the time the density current was initiated, because the mass flux of sustained explosive eruptions typically increases from the initial convective phase to the initiation of pyroclastic fountaining and generation of pyroclastic density currents (Sparks et al., 1978; Bursik and Woods, 1996). During t_1 the density current reached 6 km from source (Fig. 2), from which, using the model curves of Bursik and Woods (1996) (Table DR3), we estimate that the mass flux was ~2 × 10^8 kg/s. The gradual increase in runout distance as revealed in Figure 3, together with the gradual inundation of topographic highs from t_1 to t_5 (Fig. 2), indicate that this mass flux then continued to increase significantly.

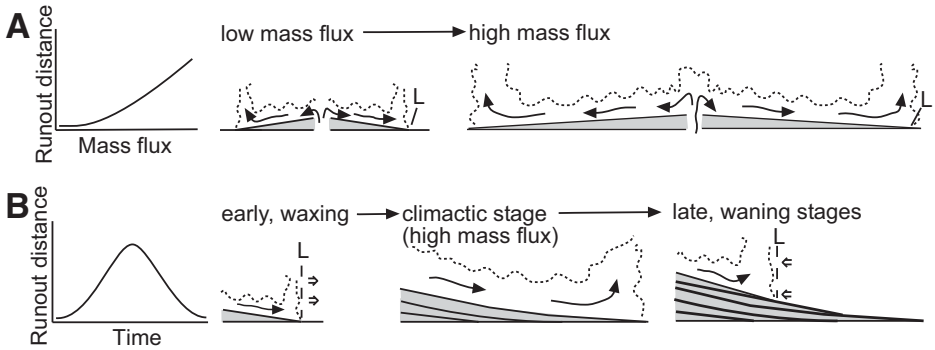

Figure 4. Eruptive mass flux versus current runout distance (from Bursik and Woods, 1996). A: Radial, sustained density current at low mass flux travels short distance before lift-off point (L), where current lofts following density loss by deposition and mixing dilution during transport (depletive flow). At higher mass fluxes, current travels further from source. B: Emplacement of Green Tuff density current reconstructed: leading edge advances during initial stages of waxing mass flux, to climax (when runout distance peaks), followed by leading edge retreat during waning stages. Resultant deposit (gray; black lines are entrachrons) has diachronous base and top and records current evolution with time and space.

Although the successive eruptive mass fluxes for t_2–t_8 cannot be quantified because the current entered the sea, a dramatic increase toward peak flow conditions (t_6) is indicated by the thin, topography-draping, low-aspect-ratio nature of the deposit (aspect ratio 1:3125). After the climactic phase, the gradually decreasing runout distance together with the gradual retraction of the current from topographic highs (t_7–t_8; Figs. 2 and 3) are inferred to record the subsequent waning of the eruptive mass flux to less than it was during t_1, until the eruption eventually ceased (Fig. 4).

From the model curves of Bursik and Woods (1996), the approximate duration of the Green Tuff current would have been ≤~1.5 h (Table DR3), and, if of roughly equal duration, each time slice would represent something on the order of ~11 min, a precision rarely achieved in stratigraphy. Irrespective of the absolute values, the temporal evolution and changing distribution of the Green Tuff density current has been revealed for the first time. This high-resolution approach could be applied to other catastrophic event deposits. In modeling the behavior and runout distances of hazardous extensive pyroclastic density currents, consideration of changing conditions during prolonged flow should prove instructive, particularly given the increasing appreciation that larger catastrophic density currents are prolonged rather than quasi-instantaneous phenomena (Simpson, 1997; Kneller and McCaffrey, 2003).

ACKNOWLEDGMENTS

We acknowledge Natural Environment Research Council studentship grant NER/S/A/2006/14156, and assistance from N. Marsh (XRF), S. Hammond (LA-ICP-MS), and R. Wilson (EMP). Thanks to Peter Kokelaar, Ian Kane, and two anonymous reviewers for helpful comments.

REFERENCES CITED

Baas, J.H., Van Kesteren, W., and Postma, G., 2004, Deposits of depletive high-density turbidity currents: A flume analogue of bed geometry, structure and texture: Sedimentology, v. 51, p. 1053–1088, doi:10.1111/j.1365-3091.2004.00660.x.

Bachmann, O., and Bergantz, G.W., 2008, Deciphering magma chamber dynamics from styles of compositional zoning in large silicic ash flow sheets: Reviews in Mineralogy and Geochemistry, v. 69, p. 651–674, doi:10.2138/rmg.2008.69.17.

Branney, M.J., and Brown, R.J., 2011, Impactoclastic density current emplacement of terrestrial meteorite-impact ejecta and the formation of dust pellets and accretionary lapilli: Evidence from Stac Fada, Scotland: The Journal of Geology, v. 119, p. 275–292, doi:10.1086/659147.

Branney, M.J., and Kokelaar, B.P., 1997, Giant bed from a sustained catastrophic density current flowing over topography: Acatlán ignimbrite, Mexico: Geology, v. 25, p. 115–118, doi:10.1130/0091-7613(1997)025<0115:GBFASC>2.3.CO;2.

Branney, M.J., and Kokelaar, B.P., 2002, Pyroclastic density currents and the sedimentation of ignimbrites: Geological Society of London Memoir 27, 150 p.

Branney, M.J., Barry, T.L., and Godchaux, M., 2004, Sheathfolds in rheomorphic ignimbrites: Bulletin of Volcanology, v. 66, p. 485–491, doi:10.1007/s00445-003-0332-8.

Brown, R.J., and Branney, M.J., 2004, Bypassing and diachronous deposition from pyroclastic density currents: Evidence from a giant regressive bedform (Poris Formation, Tenerife): Geology, v. 32, p. 445–448, doi:10.1130/G20188.1.

Brown, R.J., and Branney, M.J., 2013, Internal flow variations and diachronous sedimentation within extensive, sustained, density-stratified pyroclastic density currents flowing down gentle slopes, as revealed by the internal architectures of ignimbrites on Tenerife: Bulletin of Volcanology, v. 75, 727, doi:10.1007/s00445-013-0727-0.

Bursik, M.I., and Woods, A.W., 1996, The dynamics and thermodynamics of volcanic ash flows: Bulletin of Volcanology, v. 58, p. 175–193, doi:10.1007/s004450050134.

Carrasco-Núñez, G., and Branney, M.J., 2005, Progressive assembly of a massive layer of ignimbrite with a normal-to-reverse compositional zoning: The Zaragoza ignimbrite of central Mexico: Bulletin of Volcanology, v. 68, p. 3–20, doi:10.1007/s00445-005-0416-8.

Dade, W.B., and Huppert, H.E., 1996, Emplacement of the Taupo ignimbrite by a dilute turbulent flow: Nature, v. 381, p. 509–512, doi:10.1038/381509a0.

Fierstein, J., and Wilson, C.J.N., 2005, Assembling an ignimbrite: Compositionally defined eruptive packages in the 1912 Valley of Ten Thousand Smokes ignimbrite, Alaska: Geological Society of America Bulletin, v. 117, p. 1094–1107, doi:10.1130/B25621.1.

Kelfoun, K., 2011, Suitability of simple rheological laws for the numerical simulation of dense pyroclastic flows and long runout volcanic avalanches: Journal of Geophysical Research, v. 116, B08209, doi:10.1029/2010JB007622.

Kneller, B.C., and Branney, M.J., 1995, Sustained high-density turbidity currents and the deposition of thick massive sands: Sedimentology, v. 42, p. 607–616, doi:10.1111/j.1365-3091.1995.tb00395.x.

Kneller, B.C., and McCaffrey, W.D., 2003, The interpretation of vertical sequences in turbidite beds: The influence of longitudinal flow structure: Journal of Sedimentary Research, v. 73, p. 706–713, doi:10.1306/031103730706.

Mahood, G.A., and Hildreth, W., 1986, Geology of the peralkaline volcano at Pantelleria, Strait of Sicily: Bulletin of Volcanology, v. 48, p. 143–172, doi:10.1007/BF01046548.

Meyer, C.M., Jébrak, D., Stöffler, D., and Riller, U., 2011, Lateral transport of suevite inferred from 3D shape-fabric analysis: Evidence from the Ries impact crater, Germany: Geological Society of America Bulletin, v. 123, p. 2312–2319, doi:10.1130/B30393.1.

Murcia, H.F., Sheridan, M.F., Macías, J.L., and Cortés, G.P., 2010, TITAN2D simulations of pyroclastic flows at Cerro Machín Volcano, Colombia: Hazard implications: Journal of South American Earth Sciences, v. 29, p. 161–170, doi:10.1016/j.jsames.2009.09.005.

Orsi, G., and Sheridan, M.F., 1984, The Green Tuff of Pantelleria: Rheoignimbrite or rheomorphic fall?: Bulletin of Volcanology, v. 47, p. 611–626, doi:10.1007/BF01961230.

Pirmez, C., and Imran, J., 2003, Reconstruction of turbidity currents in a meandering submarine channel: Marine and Petroleum Geology, v. 20, p. 823–849, doi:10.1016/j.marpetgeo.2003.03.005.

Plink-Björklund, P., Steel, R. and Mellere, D., 2001, Turbidite variability and architecture of sand-prone, deep-water slopes: Eocene clinoforms in the Central Basin, Spitsbergen: Journal of Sedimentary Research, v. 71, p. 895–912.

Roche, O., 2012, Depositional processes and gas pore pressure in pyroclastic flows: An experimental perspective: Bulletin of Volcanology, v. 74, p. 1807–1820, doi:10.1007/s00445-012-0639-4.

Self, S. 2006 The effects and consequences of very large explosive volcanic eruptions: Philosophical Transactions of the Royal Society A, v. 364, p. 2073–2097.

Simpson, J.E., 1997, Gravity currents in the environment and the laboratory (2nd edition): Cambridge, UK, Cambridge University Press, 244 p.

Sparks, R.S.J., Wilson, L., and Hulme, G., 1978, Theoretical modeling of the generation, movement, and emplacement of pyroclastic flows by column collapse: Journal of Geophysical Research, v. 83, p. 1727–1739, doi:10.1029/JB083iB04p01727.

Williams, R., 2010, Emplacement of radial pyroclastic density currents over irregular topography: The chemically-zoned, low aspect-ratio Green Tuff ignimbrite, Pantelleria, Italy [Ph.D. thesis]: Leicester, UK, University of Leicester, 224 p., doi:10.6084/m9.figshare.789054.

Witham, C.S., 2005, Volcanic disasters and incidents: A new database: Journal of Volcanology and Geothermal Research, v. 148, p. 191–233, doi:10.1016/j.jvolgeores.2005.04.017.

Woods, A.W., Bursik, M.I., and Kurbatov, A.V., 1998, The interaction of ash flows with ridges: Bulletin of Volcanology, v. 60, p. 38–51, doi:10.1007/s004450050215.

Manuscript received 12 June 2013
Revised manuscript received 8 October 2013
Manuscript accepted 14 October 2013

Printed in USA